Cell Tissue Res (2010) 340:159–168
DOI 10.1007/s00441-010-0927-2

REGULAR ARTICLE

Aquaporin-1 in blood vessels of rat circumventricular organs

Alan J. Wilson · Colin J. Carati · Bren J. Gannon · Rainer Haberberger · Tim K. Chataway

Received: 5 November 2009 / Accepted: 12 January 2010 / Published online: 23 February 2010

Abstract Although the water channel protein aquaporin-1 (AQP1) is widely observed outside the rat brain in continuous, but not fenestrated, vascular endothelia, it has not previously been observed in any endothelia within the normal rat brain and only to a limited extent in the human brain. In this immunohistochemical study of rat brain, AQP1 has also been found in microvessel endothelia, probably of the fenestrated type, in all circumventricular organs (except the subcommissural organ and the vascular organ of the lamina terminalis): in the median eminence, pineal, subfornical organ, area postrema and choroid plexus. The majority of microvessels in the median eminence, pineal and choroid plexus, known to be exclusively fenestrated, are shown to be AQP1-immunoreactive. In the subfornical organ and area postrema in which many, but not all, microvessels are fenestrated, not all microvessels are AQP1-immunoreactive. In the AQP1-immunoreactive microvessels, the AQP1 probably facilitates water movement between blood and interstitium as one component of the normal fluxes that occur in these specialised sensory and secretory areas. AQP1-immunoreactive endothelia have also been seen in a small population of blood vessels in the cerebral parenchyma outside the circumventricular organs, similar to other observations in human brain. The proposed development of AQP1 modulators to treat various brain pathologies in which AQP1 plays a deleterious role will necessitate further work to determine the effect of such modulators on the normal function of the circumventricular organs.

Keywords Aquaporins · Circumventricular organs · Blood-brain barrier · Fenestrated capillaries · Endothelia · Rat (Sprague Dawley)

Introduction

Aquaporin water channel proteins, of which currently 13 mammalian types have been identified, have a wide distribution throughout the body and have been shown to play a significant role in normal and abnormal water movements (Agre et al. 2002); this includes the brain (Zador et al. 2007; Tait et al. 2008). Aquaporins-1, 4 and 9 (AQP1, AQP4, AQP9) are the predominant aquaporins in the brain (Badaut et al. 2002), although aquaporins-2, 3 and 7 (AQP2, AQP3, AQP7) are present to a lesser extent (Mobasheri et al. 2005; Shin et al. 2006). AQP1 has long been known to be present on the apical plasma membrane of the choroid plexus epithelium (Nielsen et al. 1993), where it is significantly involved in the production of cerebrospinal fluid (CSF; Oshio et al. 2005).

Within the rat brain, AQP1 is not normally expressed in the capillary endothelial cells that maintain the blood-brain barrier (BBB), although these cells retain a capacity to express AQP1 that seems to be suppressed by the subjacent perivascular astrocytic endfeet (Dolman et al. 2005). However, a few AQP1-immunoreactive blood vessels have been observed in normal human brain, with significant AQP1 upregulation in microvascular endothelia in high-grade astrocytomas

Bren J. Gannon died 13/10/09.

This work was supported by a Flinders Institute for Health and Medical Research Competitive Research Grant.

A. J. Wilson (✉) · C. J. Carati · B. J. Gannon · R. Haberberger
Department of Anatomy and Histology, Centre for Neuroscience, School of Medicine, Flinders University, Bedford Park, SA 5042, Australia
e-mail: Alan.Wilson@flinders.edu.au

T. K. Chataway
Department of Human Physiology, Centre for Neuroscience, School of Medicine, Flinders University, Bedford Park, SA, Australia

(Saadoun et al. 2002). Outside the rat brain, AQP1 is widely expressed in the plasma membranes of continuous capillary endothelia and of non-vascular endothelia throughout the body: in cardiac, skeletal and smooth muscle capillary beds, in mammary glands, in bronchial, tracheal and nasopharyngeal capillary beds and in descending vasa recta in the kidney (Nielsen et al. 1993, 1995, 1997; Verkman 2006). In contrast to continuous capillary endothelia, AQP1 appears to be absent from the plasma membranes of fenestrated capillary endothelia throughout the rat, viz., in the small intestine and colon and in the fenestrated ascending vasa recta and glomerular and peritubular capillaries of the kidney (Nielsen et al. 1993, 1995; Gannon and Carati 2003), although Nagy et al. (2002) report the presence of AQP1 in rat glomerular capillaries, which conflicts with the findings of Nielsen et al. (1993, 1995).

Although the great majority of the capillaries within the brain are of the continuous type and maintain the BBB, the small specialised regions that make up the circumventricular organs (CVOs) lie outside the BBB. The CVOs include the choroid plexus, pineal, median eminence, subfornical organ, vascular organ of the lamina terminalis (OVLT) and area postrema. The blood vessels in these regions differ from those in the rest of the brain in that they contain fenestrated and continuous muscle-type capillaries, both of which are considerably more permeable than BBB vessels (Oldfield and McKinley 2004). In this study, we report, for the first time, the presence of AQP1-immunoreactive blood vessels in the rat brain, within the CVOs. We also confirm the presence of occasional AQP1-immunoreactive blood vessels in the cerebral parenchyma outside the CVOs, as previously reported in the human brain (Saadoun et al. 2002).

Materials and methods

All experiments were carried out in accordance with the Australian Code of Conduct for the Care and Use of Animals for Scientific Purposes 2004 and with the approval of the institutional animal welfare committee.

Young adult Sprague-Dawley rats (n=15, 250–350 g), of either sex, were anaesthetised with intraperitoneal ketamine (100 mg/kg; Parnell Laboratories, NSW, Australia) and xylazine (10 mg/kg; Ilium Xylazil-20, Troy Laboratories, NSW, Australia) and were perfused transcardially with heparinised (10 U/ml) saline followed by 0.1 M phosphate-buffered 4% paraformaldehyde, pH 7.4. The brain and brainstem were removed and left in fixative overnight.

Light-microscopic immunohistochemistry

Fixed brains, embedded in paraffin wax by using conventional histological techniques, were cut into 5-μm coronal or sagittal sections and mounted on glass slides. Serial sections, both coronal and sagittal, were cut through the CVOs: median eminence, subfornical organ, area postrema, OVLT and pineal. Most paraffin-embedded sections underwent antigen retrieval. Slides were immersed in Retrievit-8 target retrieval solution, viz. EDTA buffer at pH 8, containing a chaotrope (KCl) and an ion chelator (BioGenex, San Ramon, Calif., USA), briefly boiled in a microwave oven and then maintained at 100°C in a steamer for 30 min. Following antigen retrieval, rehydrated sections were incubated for 5 min in 3% aqueous hydrogen peroxide to quench endogenous peroxidase, blocked with 10% normal donkey serum (Sigma, St. Louis, Mo., USA) for 30 min and then incubated overnight at room temperature with affinity-purified polyclonal rabbit anti-AQP1 antiserum (1:200, 5 μg/ml, AQP11-A, batch 117980A10; Alpha Diagnostic, San Antonio, Tex., USA). Next day, the sections were rinsed and then incubated for 1 h at room temperature in biotin-SP-conjugated affinity-purified donkey anti-rabbit IgG (1:400; Jackson ImmunoResearch Laboratories, West Grove, Pa., USA) containing 10% normal donkey serum. Sections were then incubated for 1 h in ExtrAvidin-peroxidase (1:100, Sigma) followed by visualisation with 3,3′-diaminobenzidine (DAB) and urea hydrogen peroxide (Sigmafast tablets, Sigma) for 15 min. After brief counterstaining with haematoxylin, sections were dehydrated and mounted in organic mounting medium.

Some fixed brains were sectioned at a thickness of 50–60 μm on a vibratome (TPI, St. Louis, Mo, USA). Sections underwent antigen retrieval, as previously described, and were processed as described by Llewellyn-Smith and Minson (1992). In brief, sections were washed in 50% ethanol for 3 h, blocked with 10% normal donkey serum and incubated for 96 h in polyclonal AQP1 antiserum (1:5000; Alpha Diagnostic) followed by 96 h in biotin-SP-conjugated affinity-purified donkey anti-rabbit IgG (1:400; Jackson) and 96 h in ExtrAvidin-peroxidase (1:1500; Sigma). Peroxidase was visualised by a standard or nickel-enhanced DAB method. The sections were then dehydrated and flat-embedded in Durcupan epoxy resin (Fluka, Buchs, Switzerland) under Aclar coverslips for light microscopy.

Sections were viewed by light microscopy and colour images were captured with a charge-coupled device digital camera (QImaging, Burnaby, BC, Canada) by using QCapture software (QImaging). Micrographs were assembled and labelled in Photoshop (Adobe Systems, San Jose, Ca., USA). Images of a 100-line/mm microscope calibration scale (Olympus, Tokyo, Japan) were obtained at corresponding magnifications and were used to derive scale markers. These were incorporated into the micrographs digitally by using Photoshop software (Adobe Systems).

Antibody specificity

The rabbit polyclonal anti-AQP1 antibody (Alpha Diagnostic) was raised against a synthetic peptide (EEYDLDADDINSR VEMKPK) representing the 19 C-terminal amino acids at positions 251–269 from rat AQP1 and was characterised by Speake et al. (2003) in Western blots of rat choroid plexus and kidney in which it identified two bands of approximately 27 kDa and 32 kDa. The same antibody identified unglycosylated (28 kDa) and glycosylated (~42 kDa) bands in rat brain microvessels and lung and in the GP8 cell line that maintains brain microvessel properties (Kobayashi et al. 2006). Dexamethasone caused up-regulation of AQP1 expression in GP8 cells, as reflected in Western blots; the upregulation was associated with increased levels of AQP1 mRNA (Kobayashi et al. 2006).

A mouse monoclonal anti-AQP1 antibody (ab9566, clone 1/22, Abcam, Cambridge, UK) was used to carry out additional immunostaining in paraformaldehyde-fixed paraffin-embedded sections in order to provide further validation of the findings with the polyclonal antibody. Sections were incubated overnight with the primary antibody (1:100) and then were incubated for 1 h in biotin-SP-conjugated affinity-purified donkey anti-mouse IgG (1:400; Jackson). All primary and secondary antisera contained 10% normal donkey serum as a blocking agent. Further processing was as described earlier.

The mouse monoclonal anti-AQP1 antibody (Abcam) was prepared against a synthetic peptide (GQVEEYDLDD DINSRVEMKPK) corresponding, except for one amino acid, to the 21 C-terminal amino acids at positions 249–269 from rat AQP1 and was thoroughly characterised by Nagy et al. (2002) by using enzyme-linked immunosorbent assay, dot-blot, Western blot, immunohistochemistry and reverse transcription with the polymerase chain reaction (RT-PCR).

As a further check on the specificity of the AQP1 polyclonal antibody, formalin-fixed cryostat sections of brains from AQP1-knockout and wild-type mice were kindly donated by Dr. Ole Petter Ottersen (University of Oslo), with the permission of Dr. Alan Verkman (University of California) and Dr. Walter Boron (Yale University). For immunofluorescent staining, these sections were blocked with 10% normal donkey serum (Sigma) for 30 min and then incubated overnight at room temperature with affinity-purified polyclonal rabbit anti-AQP1 antiserum (1:200, 5 μg/ml; Alpha Diagnostic). Next day, sections were rinsed, incubated for 2 h at room temperature with Cy3-conjugated affinity-purified polyclonal donkey anti-rabbit IgG (1:200; Jackson) and mounted in aqueous mountant. AQP1-knockout and wild-type sections were processed simultaneously for immunofluorescence staining.

Control sections were incubated: (1) with secondary, but not primary, antiserum; (2) without primary and secondary antisera; (3) with non-immune rabbit serum at the same concentration as the primary antiserum; (4) with AQP1 antiserum quenched overnight at 4°C with a 10-fold excess of its immunogenic AQP1 peptide antigen (50 μg/ml, Alpha Diagnostic). Many brain sections included the choroid plexus, which served as an internal positive control for AQP1.

RT-PCR analysis

Sprague-Dawley rats (n=7) were killed by anaesthetic overdose and then their brains were removed and placed on ice. The pineal, median eminence, subfornical organ, area postrema and choroid plexus were dissected, with kidney tissue being taken as a positive control. The tissue samples were snap-frozen in liquid nitrogen and total RNA was isolated according to the recommended protocol (Qiagen, Doncaster, Australia). Contaminating DNA was removed by using on-column DNase digestion (Qiagen). Equal amounts of RNA were reverse-transcribed with the iScript cDNA synthesis kit (Bio-Rad Laboratories, Regents Park, Australia) according to the recommended protocol. For the PCR, $MgCl_2$ (2 mM), 1 μl dNTP (200 μM each), 1.25 U HotStarTaq Plus DNA Polymerase (all reagents from Qiagen) and 20 μM primer pairs directed against rat aquaporin 1 (GI: 6978526, forward CCGAGACT TAGGTGGCTCAG, reverse TCATGCGGTCTG TAAAGTCG) and the house-keeping gene D-glyceraldehyde-3-phosphate dehydrogenase (GAPdH; GI: 89573920, forward CGTCTTCACCACCATGGAGA, reverse CGGCCATCACGCCACAGCTT; Sigma-Proligo, Lismore, Australia) were mixed and cycled under the following conditions: 5 min at 95°C, 35 cycles of 30 s at 94°C, 30 s at 60°C and 30 s at 72°C followed by 7 min at 72°C. Control reactions for RT-PCR included the absence of the RT reaction before PCR and the absence of template, which was replaced by water. Control reactions showed no amplification products. The specificity of primers was confirmed by comparison of the primer sequences with known mRNA sequences by using the BLAST database (http://www.ncbi.nlm.nih.gov/BLAST/). Products were analysed by cycle-sequencing. The expected size of the amplification product was 245 bp.

Results

Light-microscopic immunohistochemistry

In paraffin-embedded sections, either with or without antigen retrieval, AQP1 staining was strongly positive on the apical membranes of the choroid plexus epithelium, as

previously reported. In addition, however, the choroid plexus microvessels showed AQP1 immunoreactivity in their endothelia (Fig. 1a). The intensity of staining of the endothelia was lower than that of the apical membranes of the epithelium, and the endothelium of choroid arterioles, identified by the presence of smooth muscle, exhibited no staining.

AQP1 immunoreactivity was found in microvessel endothelial cells in all of the CVOs examined, with the exception of the OVLT. In the pineal, AQP1 immunostaining was seen in the majority of microvessels forming the extensive vascular network in the gland (Fig. 1b). The endothelium of microvessels in the median eminence, subfornical organ and area postrema were also strongly immunostained for AQP1. The majority of vessels in the external zone of the median eminence were AQP1-positive and included capillaries and larger diameter sinusoidal vessels (Fig. 1c). Some of the stained vessels extended into the internal zone; however, vessels in the subependymal zone were not immunostained. The stained vessels continued into the infundibular stalk, where they formed a complete investment around the periphery of the stalk (Fig. 1c). In the subfornical organ and the area postrema, some, but not all, microvessels were AQP1-positive. Sagittal and coronal serial sections through the subfornical organ revealed numerous AQP1-immunoreactive microvessels in the caudal portion (Fig. 1d), although other non-immunoreactive microvessels were also observed. No AQP1-immunoreactive vessels occurred in the rostral portion of the subfornical organ (Fig. 1e), in which vascularity was much lower than in the caudal portion. The area postrema was similar to the subfornical organ, in that both AQP1-immunoreactive and non-immunoreactive microvessels were observed (Fig. 2a). In all cases of AQP1 immunoreactivity of CVO micro-

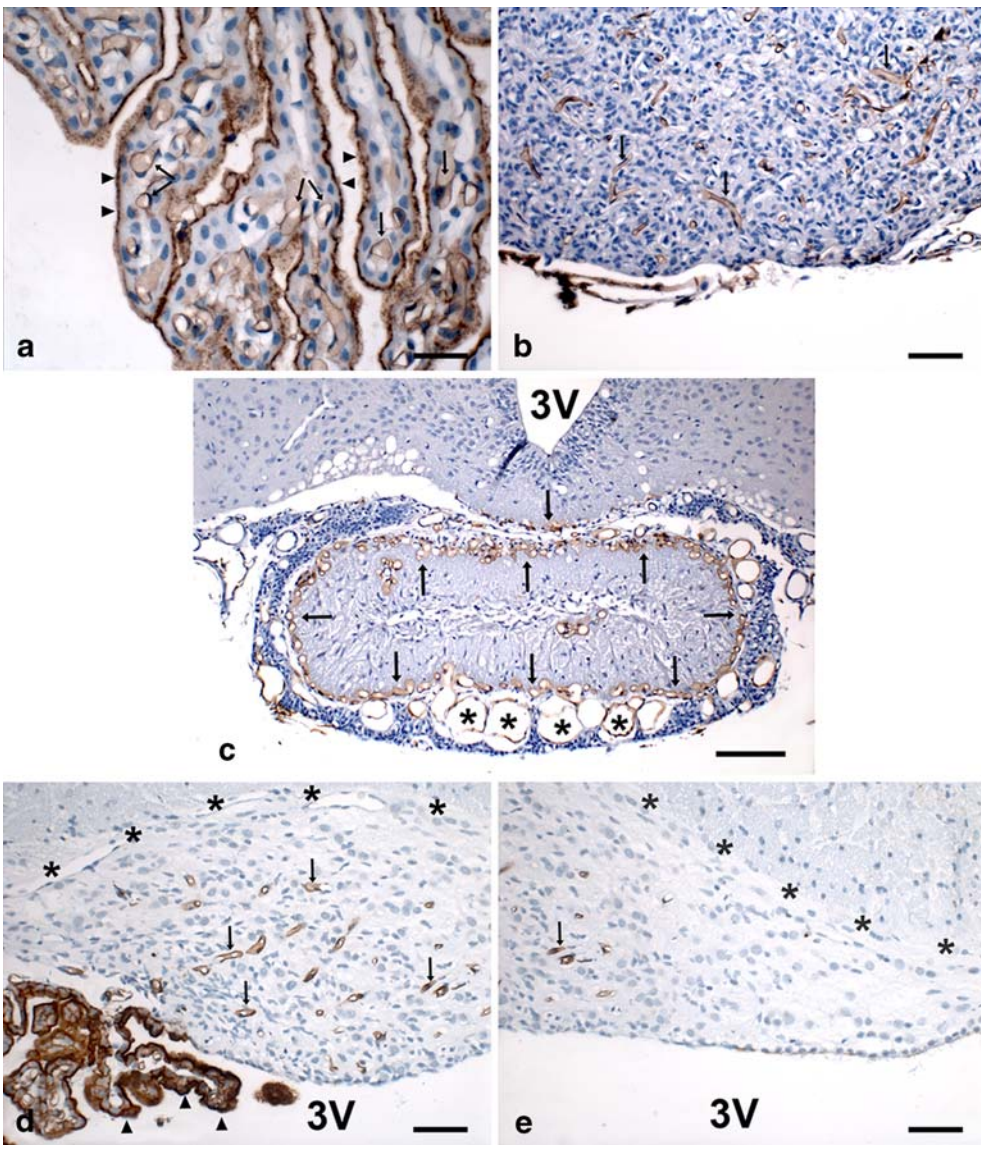

Fig. 1 Aquaporin-1 (AQP1) immunoreactivity of microvessels in rat circumventricular organ, as revealed by a polyclonal antiserum. **a** Choroid plexus: epithelial apical membranes are strongly stained (*arrowheads*), with endothelial cells of choroid microvessels also being stained, although less strongly (*arrows*). **b** Pineal: most microvessel endothelia are stained (*arrows*). **c** Median eminence: capillary (*arrows*) and sinusoidal vessel (*stars*) endothelia are stained in the median eminence and extend into the infundibular stalk, where they form a complete investment (*3V* third ventricle). Coronal section. **d**, **e** Subfornical organ: single sagittal section through the middle and caudal region (**d**) and the rostral region (**e**). Many vessels are stained in the middle and caudal region of the organ (*arrows*) but no stained vessels are present in the rostral region (*stars* superior margin of the subfornical organ). The heavily stained choroid plexus (*arrowheads*) arises adjacent to the caudal portion of the organ (*3V* third ventricle). *Bars* 25 μm (**a**), 50 μm (**b**, **d**, **e**), 100 μm (**c**)

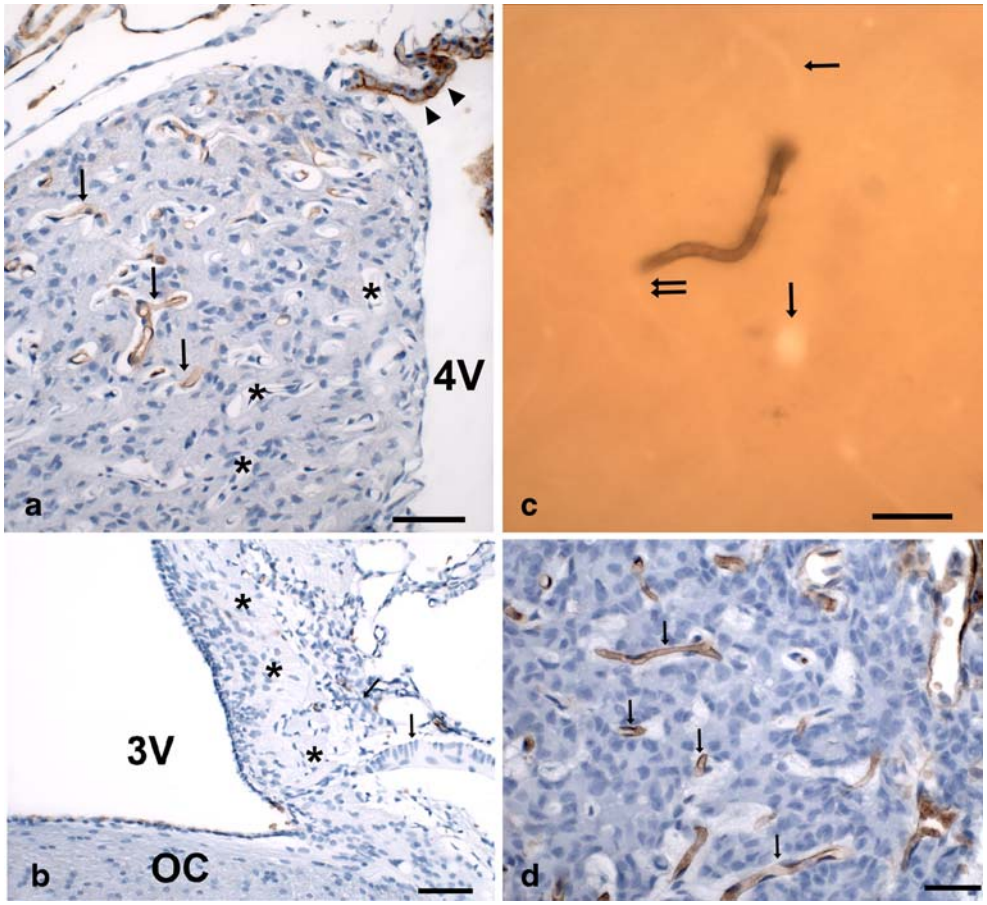

Fig. 2 AQP1 immunoreactivity of microvessels in rat circumventricular organs (**a**, **b**, **d**), by using a polyclonal (**a–c**) and a mouse monoclonal AQP1 antiserum (**d**). **a** Area postrema, sagittal section: some microvessels are stained (*arrows*), although others are unstained (*stars*). Note the stained fourth ventricular (*4V*) choroid plexus epithelium (*arrowheads),* arising from the anterosuperior aspect of the area postrema. **b** OVLT, sagittal section: no stained microvessels are seen, despite their abundance in the adjacent median eminence and subfornical organ of the same section. Arterioles (*arrows*) enter from the anterior aspect to supply the capillary bed within the OVLT parenchyma (*stars*). The optic chiasma (*OC*) forms the floor of the third ventricle (*3V*). A few residual AQP1-immunoreactive erythrocytes can be seen. **c** Cerebral cortex: occasional AQP1-immunoreactive microvessels are present, although the vast majority are unstained (*arrows*). At the *double arrow*, the stained vessel segment is continuous with an unstained segment. Vibratome section (50 μm thick). **d** Pineal: a monoclonal AQP1 antiserum stains many microvessels (*arrows*), similar to the result obtained with the polyclonal antiserum used predominantly in this study (cf. Fig. 1b). Similar results were obtained with the monoclonal antiserum in the other circumventricular organs. *Bars* 25 μm (**b**, **d**), 50 μm (**a**, **c**)

vessels, the staining was endothelial and not perivascular. Similar immunoreactivity was observed with or without antigen retrieval. No staining was observed in OVLT microvessels (Fig. 2b), although in the same sagittal sections, staining was seen in microvessels of the adjacent median eminence and subfornical organ.

Occasional AQP1-immunoreactive vascular profiles were seen within the cortical parenchyma, particularly in 50-μm-thick vibratome sections. The diameters of these vessels suggested that they were mostly arterioles, although occasional vessels were observed that had a diameter consistent with capillaries (Fig. 2c). In the thick sections, AQP1-immunoreactive vessel segments were continuous with unstained segments of the same vessel or branched from unstained vessels.

Antibody specificity

In paraformaldehyde-fixed sections in which a mouse monoclonal anti-AQP1 was used as the primary antiserum, the pattern of staining was identical to that seen when using the rabbit polyclonal anti-AQP1 primary antiserum, although the intensity of staining was lower than with the polyclonal antiserum. AQP1-positive endothelial cells were seen in the median eminence, subfornical organ, area postrema, choroid plexus and pineal (Fig. 2d).

No AQP1 immunofluoresecence was seen in cryostat sections of any part of the brain of the AQP1-knockout mouse, including sections with the choroid plexus (Fig. 3a) and median eminence (Fig. 3b), when the polyclonal AQP1 antiserum was used. Under the same immunofluorescence

staining conditions, AQP1 immunoreactivity was observed on the apical membranes of epithelial cells of the choroid plexus (Fig. 3c) and in blood vessels in the median eminence (Fig. 3d) in brain sections of the wild-type mouse.

Pre-adsorption of the polyclonal AQP1 antiserum with an excess of the AQP1 peptide antigen resulted in abolition of all staining. Sections in which secondary and/or primary antisera were omitted or in which a pre-immune serum was used as the primary antiserum were unstained.

RT-PCR analysis

A distinct band of the expected size (245 bp) was seen in each of the tissue samples: choroid plexus (positive control), area postrema, pineal, median eminence and subfornical organ (Fig. 4). No amplification product was seen in the controls.

Discussion

Until recently, AQP1 in the rat brain was considered to be restricted to the plasma membranes of the epithelial cells of the choroid plexus, where it has been shown to play a role in CSF production (Oshio et al. 2005). We now report the immunolocalisation of AQP1 in capillary endothelia in most CVOs (choroid plexus, pineal, median eminence, subfornical organ, area postrema, but not OVLT) in the rat brain and in endothelia of a small number of vessels in the cerebral parenchyma. Our findings are consistent with a number of other recent reports. Although the strong AQP1 immunoreactivity of choroid plexus epithelia has long been noted (Nielsen et al. 1993), AQP1 immunreactivity of the endothelia of the human choroid plexus microvasculature has been reported only recently (Longatti et al. 2004, 2006; Praetorius and Nielsen 2006). As is the case with our current observations in the rat choroid plexus endothelia, this delayed recognition has probably occurred because, particularly with immunofluorescence techniques, the high intensity of epithelial AQP1 immunostaining in combination with the compact and convoluted nature of the choroid plexus tissue tends to mask the less intense endothelial staining. Endothelial cells that are immunoreactive for AQP1 have been reported recently in the rat pituitary gland (Kuwahara et al. 2007); this is in agreement with our observations in the median eminence. Our observation of a small number of parenchymal (i.e. non-CVO) blood vessels with AQP1-immunoreactive endothelia in rat brain is consistent with similar observations in normal human brain (Saadoun et al. 2002).

The CVOs are a group of specialised brain regions in the walls of the lateral, third and fourth ventricles, all of which, apart from the atypical subcommissural organ, contain fenestrated blood vessels that are highly permeable and place the CVOs outside the BBB (for reviews, see Gross

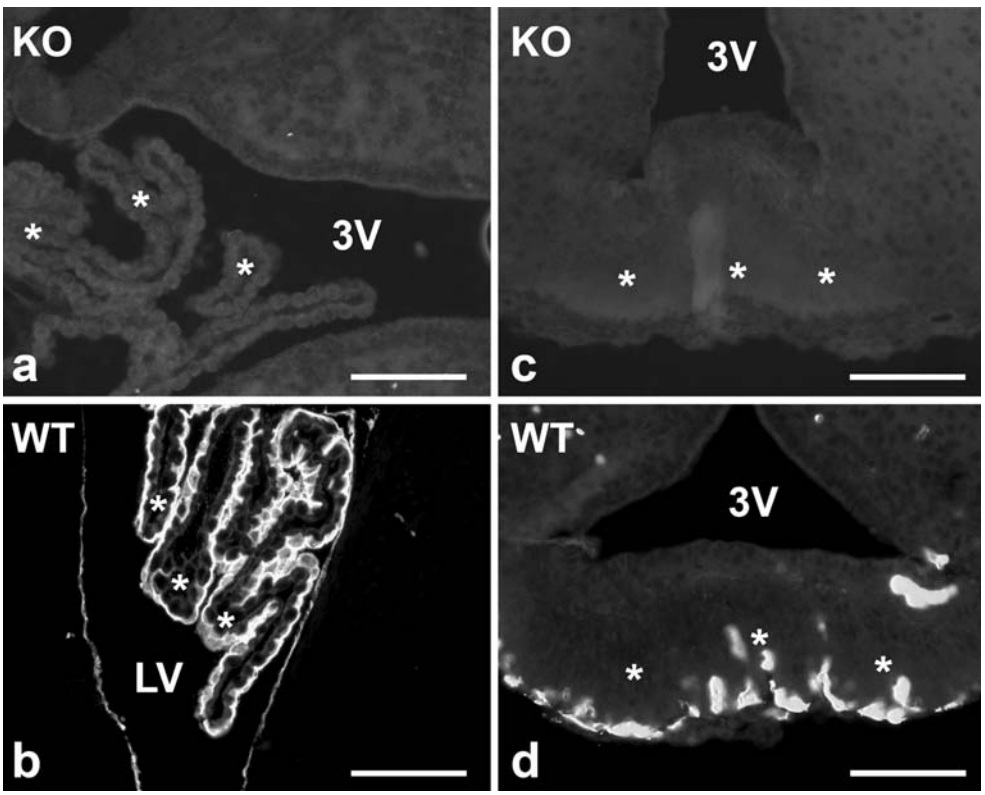

Fig. 3 AQP1 immunofluorescence in cryosections of the circumventricular organs of AQP1-knockout (*KO*, **a**, **c**) and wild-type (*WT*, **b**, **d**) mouse brain, to check for antibody specificity. **a** In the AQP1-KO mouse brain, staining of the choroid plexus epithelium (*stars*) is lacking, compared with the strong staining in the WT mouse choroid epithelium (*stars* in **b**). No immunofluorescence is found in the median eminence (*stars*) of the AQP1-KO mouse in **c**, compared with the strong immunofluorescence in blood vessels in the WT median eminence (*stars* in **d**). KO and WT sections were immunostained simultaneously (*3V* third ventricle, *LV* lateral ventricle). *Bars* 100 μm

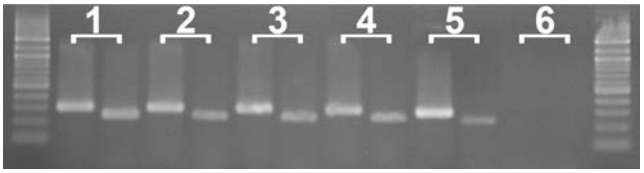

Fig. 4 Reverse transcription with polymerase chain reaction (RT-PCR) analysis of AQP1 and D-glyceraldehyde-3-phosphate dehydrogenase (GAPdH) transcript expression in rat brain. For each pair of lanes, the *left lane* is AQP1 and the *right lane* is GAPdH. Bands were seen for pineal (*lane pair 1*), median eminence (*lane pair 2*), subfornical organ (*lane pair 3*), choroid plexus (positive control, *lane pair 4*), area postrema (*lane pair 5*). No band was seen for the kidney control (*lane pair 6*) with omission of the RT step to control for DNA contamination

1992; Oldfield and McKinley 2004). Their highly permeable vessels allow them to play important regulatory roles, including cardiovascular and fluid homeostasis, and endocrine regulation. All the CVOs that have been investigated in this study, with the exception of the OVLT, contain AQP1-immunoreactive endothelial cells: the choroid plexus, pineal, median eminence, subfornical organ and area postrema. In the choroid plexus, the pineal and external zone of the median eminence, where the portal plexus is composed of both capillaries and larger (>7.5 μm diameter) sinusoids (Shaver et al. 1992), all microvessels are fenestrated (Type III; Marchesi and Barrnett 1964) and are surrounded by a large perivascular space (Gross 1992; Oldfield and McKinley 2004). Most, if not all, microvessel endothelia in these areas are AQP1-immunoreactive. With the exception of the contradictory findings in renal glomeruli (Nielsen et al. 1993, 1995; Nagy et al. 2002), these capillaries are so far the only fenestrated capillaries in the rat to be definitively shown to be AQP1-positive; all other fenestrated capillaries in the rat outside the brain appear to be AQP1-negative, although many continuous capillaries outside the brain are AQP1-positive (Nielsen et al. 1993).

The subfornical organ contains a number of morphologically and functionally distinct zones and subregions, with a heterogeneous distribution of capillary densities and types (Sposito and Gross 1987; Shaver et al. 1990; Oldfield and McKinley 2004). The rostral zone of the subfornical organ, in marked contrast to the rest of the organ, is an area of low vascular density and permeability, because of the exclusive presence of Type II vessels (Marchesi and Barrnett 1964) that morphologically and functionally resemble BBB vessels in the brain parenchyma (Bouchaud et al. 1989; Sposito and Gross 1987; Gross 1992), i.e. they are continuous, with no perivascular space. In the central and caudal ventromedial areas, capillary density and permeability are high and Type I (continuous, muscle-type, narrow perivascular space; Marchesi and Barrnett 1964), Type II and Type III capillaries are all present (Bouchaud et al. 1989; Shaver et al. 1990). Since we have observed no AQP1-immunoreactive vessels in the rostral zone, where only Type II vessels are found, but as we have found numerous stained vessels, together with unstained vessels, in the central and caudal regions of the organ, then the stained vessels are probably not Type II. In view of the finding that most, if not all, fenestrated (Type III) vessels in the choroid plexus, pineal and median eminence are AQP1-immunoreactive, all the stained vessels within the subfornical organ are probably also fenestrated and the unstained vessels in the central and caudal regions are likely to be Types I and II.

The area postrema is characterised by a high density of Type I and Type III vessels, which accounts for the high vascular permeability of the area; the vessels include capillaries (<7.5 μm diameter) and larger (>7.5 μm diameter) sinusoids (Shaver et al. 1991; Gross 1992). All vessels have perivascular spaces, with capillaries and sinusoids sometimes sharing the same perivascular space (Shaver et al. 1991). Some, but not all, of the vessels in the area postrema have been found to be AQP1-immunoreactive. For similar reasons as those put forward for the subfornical organ, AQP1-immunoreactive vessels are probably fenestrated (Type III).

In the median eminence and pineal, the presence of AQP1 in the majority of microvessels probably assists with the rapid movement of neurohormones into the blood in these two areas. The AQP1 immunoreactivity in the fenestrated microvessels of the choroid plexus is likely to facilitate water movement from the blood into the choroid parenchyma as a component of CSF production. In AQP1-knockout mice, CSF production has been found to be reduced by 20%–25% (Oshio et al. 2005). Although this reduction is assumed to be attributable solely to the deletion of AQP1 on the apical membranes of choroid plexus epithelia, a deletion of AQP1 might also have occurred in the microvessels of the choroid plexus and this may have had some effect on the observed reduction in CSF production. The presence of AQP1 in microvessels in the subfornical organ and area postrema probably facilitates water movement from the blood into these organs as part of their role in monitoring the composition of the blood. Since nerve terminals containing neuroactive peptides have been observed within the perivascular spaces of fenestrated vessels in the subfornical organ, area postrema and median eminence, AQP1 in these vessels most probably also participates in the neurosecretion of peptides from brain to blood (Oldfield et al. 1989; Oldfield and McKinley 2004).

The observation of AQP1-immunoreactive endothelial cells in microvessels of the majority of the CVOs and the likelihood that the stained vessels belong to the fenestrated category, with large perivascular spaces, raise the question as to why no AQP1-immunoreactive vessels have been

found in the OVLT, which is known to contain a dense plexus of fenestrated vessels (Krisch et al. 1987; Yamaguchi et al. 1993), when all the other CVOs contained AQP1-immunoreactive vessels, some of which are known to be, and the rest hypothesised to be, fenestrated? The OVLT has a number of characteristics that suggest that its fenestrated vessels differ from those in the other CVOs. The OVLT has been observed to have two separate vascular beds, both containing fenestrated capillaries: a superficial vascular plexus that is impermeable to horseradish peroxidase, and a deep vascular plexus that is permeable to horseradish peroxidase (Krisch et al. 1987). In the murine brain, tight-junction-associated protein ZO-1 has been detected in all OVLT capillary endothelia, in a continuous linear form, similar to the pattern seen in capillaries in brain areas with an intact BBB (Petrov et al. 1994). In the subfornical organ, median eminence and area postrema, by contrast, the pattern of ZO-1 staining is different, with few ZO-1-labelled capillaries or capillaries with discontinuous punctate ZO-1 labelling (Petrov et al. 1994; Norsted et al. 2008; Maolood and Meister 2009).

The particular features of cerebral microvessels characteristic of the BBB phenotype are known to be induced by the surrounding cells, especially the astrocytic glia that are closely apposed to the endothelial cells (Abbott et al. 2006). Bouchaud et al. (1989) have observed that, in the subfornical organ and choroid plexus, the more distant that astrocytic processes lie from the vessels, the greater is their vascular permeability, i.e. the less they maintain the BBB phenotype. In the subfornical organ, perivascular spaces range from nonexistent (rostral Type II vessels) to small (caudal Type I vessels) to large (caudal Type III vessels) and, in the choroid plexus (Type III vessels), astrocytes are absent; permeability is ranked Type III>Type I >>Type II (Bouchaud et al. 1989). Astrocytes have been proposed to release signals that suppress the expression of endothelial characteristics such as fenestrations and endothelial vesicles that are associated with high vascular permeability, so that vessels with large perivascular spaces separating them from the astrocytic influence, or choroid vessels with no astrocytic presence, are released from the inhibitory influence (Bouchaud et al. 1989). In a similar fashion, Dolman et al. (2005) have recently provided evidence that the perivascular astrocytic investment of brain endothelia normally suppresses the expression of AQP1 in these vessels, since it is widely expressed in the endothelium of non-brain continuous capillaries (Nielsen et al. 1993, 1995, 1997; Verkman 2006). Removal of the astrocytic suppressive influence leads to the up-regulation of AQP1 expression in brain microvessel endothelial cells in culture (Dolman et al. 2005). An enlarged perivascular space or the lack of close astrocytic investment might therefore be expected to lead to a reduction in the astrocytic suppression of AQP1 expression in the endothelium. In this study, we have demonstrated that both fenestrated (Type III) microvessels with large perivascular spaces in the pineal and median eminence and fenestrated choroid plexus microvessels with no astrocytic presence are AQP1-immunoreactive. We hypothesise that the AQP1-immunoreactive vessels in the subfornical organ and area postrema are also fenestrated vessels with large perivascular spaces. Although the release from astrocytic suppression because of large perivascular spaces might be responsible for the loss of the BBB phenotype and increased permeability of fenestrated vessels in the CVOs, as postulated by Bouchaud et al. (1989), and whereas such release causes the up-regulation of AQP1 in cultured BBB phenotype endothelial cells (Dolman et al. 2005), these are not sufficient to explain the expression of AQP1 in fenestrated CVO endothelia. This is because fenestrated vessels outside the brain are not subjected to any astrocytic influence and yet do not normally express AQP1 in the rat (Nielsen et al. 1993, 1995; Gannon and Carati 2003). The expression of AQP1 in fenestrated CVO endothelia may therefore be attributable to the action of stimulatory factors within the brain, possibly localised within the CVOs themselves. Lack of a localised stimulatory factor in the OVLT may be the reason that the fenestrated vessels in this CVO are not AQP1-immunoreactive, in contrast to the other CVOs investigated.

A number of additional steps have been used to check the validity of the results and the specificity of the polyclonal AQP1 antiserum. A mouse monoclonal AQP1 antiserum raised against a similar, but slightly longer, C-terminal AQP1 peptide, produces an identical, although less intense, pattern of AQP1 immunoreactivity to that found with the polyclonal antibody. The RT-PCR technique has been applied to tissue samples from all CVOs in which AQP1 immunoreactivity has been identified and has yielded the expected amplification product in each case. In the case of the subfornical organ and area postrema, however, this cannot be interpreted as unequivocal evidence of AQP1 mRNA presence specific to the endothelial cells in these areas. The origins of the third and fourth ventricular choroid plexus are closely associated with these two areas, respectively, and although care has been taken to try to remove the choroid plexus completely during dissection, remnants might still have been present in the samples. The pineal and median eminence are remote from any possibility of choroid plexus contamination. In the choroid plexus samples, amplification product might certainly have originated from the choroid epithelium, which makes it impossible to draw any conclusions about the presence or absence of AQP1 mRNA associated with the choroid endothelia.

The rat appears to differ from the human with regard to AQP1 immunoreactivity of some fenestrated endothelia located outside the brain. In the rat kidney, AQP1 immunoreactivity is absent in the fenestrated ascending

vasa recta and glomerular and peritubular capillaries (Nielsen et al. 1993, 1995), whereas in the human kidney, the glomerular and peritubular capillaries are AQP1-immunoreactive (Maunsbach et al. 1997). This raises the possibility that our current findings in the rat brain are not reflected in the human brain, although the rat brain at least resembles the human brain with respect to AQP1 immunoreactivity in choroid plexus endothelia (Longatti et al. 2004, 2006; Praetorius and Nielsen 2006). Evidence has been obtained for the involvement of AQP1 in the brain in CSF production, in the maintenance of intracranial pressure, in cerebral oedema and in cerebral tumour migration and angiogenesis (Saadoun et al. 2002, 2005; Oshio et al. 2005; Satoh et al. 2007; Verkman et al. 2008). In view of this, the development of inhibitors of AQP1 or its expression has been proposed to yield important treatment options for a range of brain pathologies in which AQP1 upregulation has a deleterious effect (Oshio et al. 2005; Zador et al. 2007; Tait et al. 2008; Verkman et al. 2008). Therefore, a determination of whether our findings in the rat brain also apply in the human brain and, if so, whether any such inhibitory agents will have an adverse impact on the normal function of human CVOs will be of importance.

In summary, we have demonstrated the presence of AQP1 immunoreactivity in endothelial cells in microvessels in most CVO in the rat brain, including the choroid plexus, pineal, median eminence, subfornical organ and area postrema; the microvessels in the choroid plexus, pineal and median eminence are fenestrated, whereas those in the subfornical organ and area postrema are probably fenestrated. We have also demonstrated the presence of AQP1 immunoreactivity in endothelia of a small number of blood vessels in the cerebral parenchyma. These findings, if also replicated in the human brain, may have implications in the development of therapeutic agents aimed at modifying the effects of AQP1 in various brain diseases.

Acknowledgements Renata Billing provided skilled technical assistance. Dr. I.J. Llewellyn-Smith kindly provided a critical review of the manuscript.

References

Abbott NJ, Rönnbäck L, Hansson E (2006) Astrocyte-endothelial interactions at the blood-brain barrier. Nature Neurosci Rev 7:1–13

Agre P, King LS, Yasui M, Guggino WB, Ottersen OP, Fujiyoshi Y, Engel A, Nielsen S (2002) Aquaporin water channels—from atomic structure to clinical medicine. J Physiol (Lond) 542:3–16

Badaut J, Lasbennes F, Magistretti PJ, Regli L (2002) Aquaporins in brain: distribution, physiology, and pathophysiology. J Cereb Blood Flow Metab 22:367–378

Bouchaud C, Le Bert M, Dupouey P (1989) Are close contacts between astrocytes and endothelial cells a prerequisite condition of a blood-brain barrier? The rat subfornical organ as an example. Biol Cell 67:159–165

Dolman D, Drndarski S, Abbott NJ, Rattray M (2005) Induction of aquaporin 1 but not aquaporin messenger RNA in rat primary brain microvessel endothelial cells in culture. J Neurochem 93:825–833

Gannon BJ, Carati CJ (2003) Endothelial distribution of the membrane water channel molecule aquaporin-1: implications for tissue and lymph fluid physiology? Lymph Res Biol 1:55–66

Gross PM (1992) Circumventricular organ capillaries. Prog Brain Res 91:219–233

Kobayashi H, Yokoo H, Yanagita T, Satoh S, Kis B, Deli M, Niwa M, Wada A (2006) Induction of aquaporin 1 by dexamethasone in lipid rafts in immortalized brain microvascular endothelial cells. Brain Res 1123:12–19

Krisch B, Leonhardt H, Oksche A (1987) Compartments in the organum vasculosum laminae terminalis of the rat and their delineation against the outer cerebrospinal fluid-containing space. Cell Tissue Res 250:331–347

Kuwahara S, Maeda S, Tanaka K, Hayakawa T, Seki M (2007) Expression of aquaporin water channels in the rat pituitary gland. J Vet Med Sci 69:1175–1178

Llewellyn-Smith IJ, Minson J (1992) Complete penetration of antibodies into Vibratome sections after glutaraldehyde fixation and ethanol treatment: light and electron microscopy for neuropeptides. J Histochem Cytochem 40:1741–1749

Longatti PL, Basaldella L, Orvieto E, Fiorindi A, Carteri A (2004) Choroid plexus and aquaporin-1: a novel explanation of cerebrospinal fluid production. Pediatr Neurosurg 40:277–283

Longatti P, Basaldella L, Orvieto E, Dei Tos A, Martinuzzi A (2006) Aquaporin(s) expression in choroid plexus tumours. Pediatr Neurosurg 42:228–233

Maolood N, Meister B (2009) Protein components of the blood-brain barrier (BBB) in the brainstem area postrema-nucleus tractus solitarius region. J Chem Neuroanat 37:182–195

Marchesi VT, Barrnett RJ (1964) The localization of nucleosidephosphatase activity in different types of small blood vessels. J Ultrastr Res 10:103–115

Maunsbach AB, Marples D, Chin E, Ning G, Bondy C, Agre P, Nielsen S (1997) Aquaporin-1 water channel expression in human kidney. J Am Soc Nephrol 8:1–14

Mobasheri A, Wray S, Marples D (2005) Distribution of AQP2 and AQP3 water channels in human tissue microarrays. J Mol Histol 36:1–14

Nagy G, Szekeres G, Kvell K, Berki T, Németh P (2002) Development and characterisation of a monoclonal antibody family against aquaporin 1 (AQP1) and aquaporin 4 (AQP4). Pathol Oncol Res 8:115–124

Nielsen S, Smith BL, Christensen EI, Agre P (1993) Distribution of the aquaporin CHIP in secretory and resorptive epithelia and capillary endothelia. Proc Natl Acad Sci USA 90:7275–7279

Nielsen S, Pallone T, Smith BL, Christensen EI, Agre P, Maunsbach AB (1995) Aquaporin-1 water channels in short and long loop descending thin limbs and in descending vasa recta in rat kidney. Am J Physiol 268:F1023–F1037

Nielsen S, King LS, Christensen BM, Agre P (1997) Aquaporins in complex tissues. II. Subcellular distribution in respiratory and glandular tissues of rat. Am J Physiol 273:C1549–C1561

Norsted E, Gömüç B, Meister B (2008) Protein components of the blood-brain barrier (BBB) in the mediobasal hypothalamus. J Chem Neuroanat 36:107–121

Oldfield BJ, Ganten D, McKinley MJ (1989) An ultrastructural analysis of the distribution of angiotensin II in the rat brain. J Neuroendocrinol 1:121–128

Oldfield BJ, McKinley MJ (2004) Circumventricular organs. In: Paxinos G (ed) The rat nervous system, 3rd edn. Elsevier, London, pp 389–406

Oshio K, Watanabe H, Song Y, Verkman AS, Manley GT (2005) Reduced cerebrospinal fluid production and intracranial pressure in mice lacking choroid plexus water channel aquaporin-1. FASEB J 19:76–78

Petrov T, Howarth AG, Krukoff TL, Stevenson BR (1994) Distribution of the tight junction-associated protein ZO-1 in circumventricular organs of the CNS. Mol Brain Res 21:235–246

Praetorius J, Nielsen S (2006) Distribution of sodium transporters and aquaporin-1 in the human choroid plexus. Am J Physiol Cell Physiol 291:C59–C67

Saadoun S, Papadopoulos MC, Davies DC, Bell BA, Krishna S (2002) Increased aquaporin 1 water channel expression in human brain tumours. Br J Cancer 87:621–623

Saadoun S, Papadopoulos MC, Hara-Chikuma M, Verkman AS (2005) Impairment of angiogenesis and cell migration by targeted aquaporin-1 gene disruption. Nature 434:786–792

Satoh J, Tabunoki H, Yamamura T, Arima K, Konno H (2007) Human astrocytes express aquaporin-1 and aquaporin-4 in vitro and in vivo. Neuropathology 27:245–256

Shaver SW, Sposito NM, Gross PM (1990) Quantitative fine structure of capillaries in subregions of the rat subfornical organ. J Comp Neurol 294:145–152

Shaver SW, Pang JJ, Wall KM, Sposito NM, Gross PM (1991) Subregional topography of capillaries in the dorsal vagal complex of rats. I. Morphometric properties. J Comp Neurol 306:73–82

Shaver SW, Pang JJ, Wainman DS, Wall KM, Gross PM (1992) Morphology and function of capillary networks in subregions of the rat tuber cinereum. Cell Tissue Res 267:437–448

Shin I, Kim HJ, Lee JE, Gye MC (2006) Aquaporin7 expression during perinatal development of mouse brain. Neurosci Lett 409:106–111

Speake T, Freeman LJ, Brown PD (2003) Expression of aquaporin 1 and aquaporin 4 water channels in rat choroid plexus. Biochem Biophys Acta 1609:80–86

Sposito NM, Gross PM (1987) Topography and morphometry of capillaries in the rat subfornical organ. J Comp Neurol 260:34–46

Tait MJ, Saadoun S, Bell BA, Papadopoulos MC (2008) Water movements in the brain: role of aquaporins. Trends Neurosci 31:37–43

Verkman AS (2006) Aquaporins in endothelia. Kidney Int 69:1120–1123

Verkman AS, Hara-Chikuma M, Papadopoulos MC (2008) Aquaporins—new players in cancer biology. J Mol Med 86:523–529

Yamaguchi K, Morimoto A, Murakami N (1993) Organum vasculosum laminae terminalis (OVLT) in rabbit and rat: topographic studies. J Comp Neurol 330:352–362

Zador Z, Bloch O, Yao X, Manley GT (2007) Aquaporins: role in cerebral edema and brain water balance. Prog Brain Res 161:185–194